Biochemical and Biophysical Research Communications 522 (2020) 107–112

Contents lists available at ScienceDirect

Biochemical and Biophysical Research Communications

journal homepage: www.elsevier.com/locate/ybbrc

Structure and function of the two-component flavin-dependent methanesulfinate monooxygenase within bacterial sulfur assimilation

Jess Soule [a, 1], Andrew D. Gnann [a], Reyaz Gonzalez [a], Mackenzie J. Parker [b, 2], Kylie C. McKenna [c], Son V. Nguyen [c], Ngan T. Phan [a, c], Denyce K. Wicht [c, **], Daniel P. Dowling [a, *]

[a] Department of Chemistry, University of Massachusetts Boston, Boston, MA, 02125, USA
[b] Department of Chemistry, Massachusetts Institute of Technology, Cambridge, MA, 02139, USA
[c] Department of Chemistry and Biochemistry, Suffolk University, Boston, MA, 02108, USA

ARTICLE INFO

Article history:
Received 1 November 2019
Accepted 2 November 2019
Available online 18 November 2019

Keywords:
Dimethylsulfone
Methanesulfinate
Methanesulfonate
Dimethylsulfide
Global sulfur cycle
Crystal structure

ABSTRACT

Methyl sulfur compounds are a rich source of environmental sulfur for microorganisms, but their use requires redox systems. The bacterial *sfn* and *msu* operons contain two-component flavin-dependent monooxygenases for dimethylsulfone ($DMSO_2$) assimilation: SfnG converts $DMSO_2$ to methanesulfinate (MSI^-), and MsuD converts methanesulfonate (MS^-) to sulfite. However, the enzymatic oxidation of MSI^- to MS^- has not been demonstrated, and the function of the last enzyme of the *msu* operon (MsuC) is unresolved. We employed crystallographic and biochemical studies to identify the function of MsuC from *Pseudomonas fluorescens*. The crystal structure of MsuC adopts the acyl-CoA dehydrogenase fold with putative binding sites for flavin and MSI^-, and functional assays of MsuC in the presence of its oxidoreductase MsuE, FMN, and NADH confirm the enzymatic generation of MS^-. These studies reveal that MsuC converts MSI^- to MS^- in sulfite biosynthesis from $DMSO_2$.

1. Introduction

Sulfur is an essential element for life that microorganisms must assimilate from the environment, typically as sulfate [1]. In sulfate-limited environments, however, assimilation proceeds from organosulfur compounds containing stable C–S bonds, making utilization of environmental sulfur a chemical challenge [2–4]. Dimethylsulfone ($DMSO_2$) is a prevalent organosulfur compound that has two C–S bonds, the chemical precursor of which is dimethylsulfide (DMS) [5–7]. In addition to serving as a microbial source of sulfur, $DMSO_2$ can be metabolically transformed for carbon and electrons [8].

To catabolize organosulfur compounds, bacteria have evolved redox pathways including two-component flavin-dependent monooxygenases [9–12]. These systems require $FMNH^-$ and O_2, and they are found with separately encoded NAD(P)H:flavin oxidoreductases that supply $FMNH^-$ [13,14]. In the assimilation of sulfur from $DMSO_2$, methanesulfinate (MSI^-, S^{+2}) and methanesulfonate (MS^-, S^{+4}) are sequential intermediates (Fig. 1). The monooxygenase SfnG from *Pseudomonas fluorescens* Pf0-1 was shown to catalyze C–S bond cleavage of $DMSO_2$ [12], and Kertesz et al. determined that the final C–S bond in MS^- is broken by the monooxygenase MsuD to yield SO_3^{2-} and formaldehyde [3]. However, in order to complete the *in vivo* pathway for conversion of $DMSO_2$ to sulfite, the sulfur atom of MSI^- must be oxidized from S^{+2} to S^{+4}. The last gene of the *msu* operon, *msuC*, encodes a putative dehydrogenase with 42% sequence identity to the monooxygenase DszC [9], and although MsuC was reported to have a stimulating effect on the desulfonation of MS^-, the function of the enzyme remained unclear [3]. Here, we report the structure of MsuC and show by ^1H NMR spectroscopy that MsuC oxidizes MSI^- to MS^- in an $FMNH^-$-dependent manner. Our results complete the $DMSO_2$ degradation pathway of *P. fluorescens*, revealing that the microorganism uses three separate reduced flavin-dependent monooxygenases to extract sulfur from $DMSO_2$ as SO_3^{2-}.

* Corresponding author., Department of Chemistry, University of Massachusetts Boston, Boston, MA, 02125, USA.
** Corresponding author. Department of Chemistry and Biochemistry, Suffolk University, Boston, MA, 02108, USA.
E-mail addresses: dwicht@suffolk.edu (D.K. Wicht), daniel.dowling@umb.edu (D.P. Dowling).
[1] Current address: University of California Los Angeles, Los Angeles, CA 90095.
[2] Current address: New England Biolabs, 240 County Rd., Ipswich, MA 01938.

https://doi.org/10.1016/j.bbrc.2019.11.008
0006-291X/

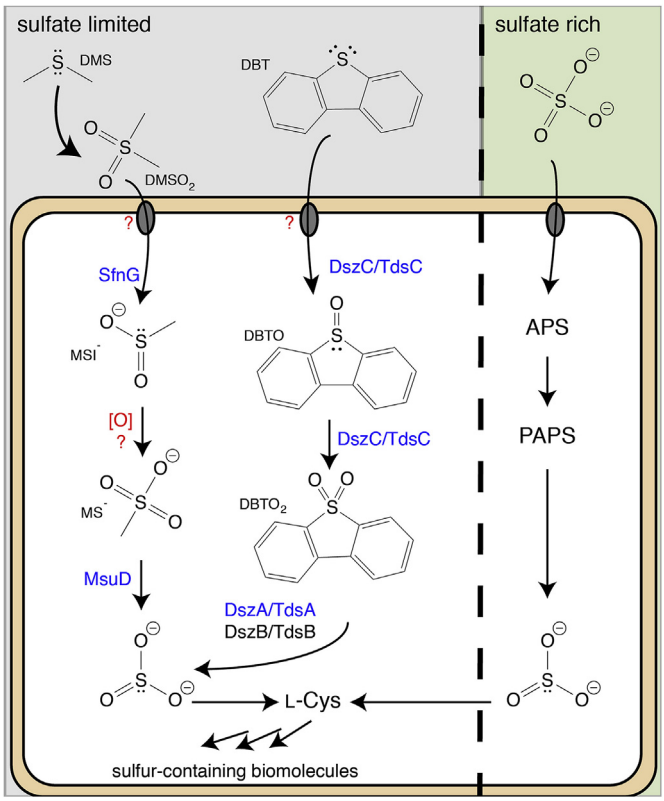

Fig. 1. Biochemical routes to sulfite from dimethylsulfide (DMS) and dibenzothiophene (DBT) in bacteria. Dimethylsulfone ($DMSO_2$) is an oxidized form of DMS that is converted to methanesulfinate (MSI^-), methanesulfonate (MS^-), and finally sulfite. In DBT metabolism, DBT is oxidized to dibenzothiophene sulfoxide (DBTO), followed by oxidation to dibenzothiophene sulfone ($DBTO_2$). Two enzymatic C–S bond cleavages convert $DBTO_2$ to sulfite. Two-component flavin-dependent monooxygenases are denoted in blue, and their flavin reductases are omitted for clarity. Transporters for $DMSO_2$ and DBT across the bacterial cell wall, represented in beige, are not known. Sulfur is standardly assimilated from sulfate by enzymatic conversion to adenosine-5′-phosphosulfate (APS), 3′-phosphoadenosine-5′-phosphosulfate (PAPS), and subsequent reduction. (For interpretation of the references to color in this figure legend, the reader is referred to the Web version of this article.)

2. Materials and methods

2.1. Construction of pPfl01_msuC

The gene Pfl01_3917 (MsuC) was amplified by PCR from *P. fluorescens* Pf0-1 genomic DNA using Phusion high fidelity DNA polymerase (New England Biolabs, NEB) and primers listed in Table S1. The amplified DNA was purified, digested with NdeI and XhoI (NEB), and ligated into similarly digested pET28a (EMD Millipore) with T4 DNA Ligase (Promega). The constructed plasmid was confirmed by sequencing.

2.2. Expression and purification

BL21(DE3) cells harboring pPfl01_*msuC* were incubated at 37 °C and 200 rpm to an OD_{600} of 0.5–0.6 and subsequently were cooled on ice before adding isopropyl-β-D-thiogalactopyranoside to 50 μM. Cultures were grown overnight at 16 °C and 200 rpm and harvested by centrifugation at 3000×*g* for 30 min at 4 °C. Cell pellets were washed with 20 mM Tris•HCl (pH 8.0) and 100 mM NaCl, frozen in liquid N_2 and stored at −80 °C.

Purification was carried out on ice or at 4 °C. The cell paste was thawed and resuspended in lysis buffer (20 mM Tris•HCl (pH 7.9), 500 mM NaCl, 5 mM imidazole) supplemented with 5 μg mL^{-1} lysozyme, 10 μg mL^{-1} DNase I, and 10 μg mL^{-1} RNase A. Cells were lysed with a French press at 14,000 psi and clarified by centrifugation at 10,000×*g* for 30 min. The cell-free extract was loaded onto a 6 mL Ni-nitrilotriacetic acid Sepharose column equilibrated in lysis buffer. The column was washed with lysis buffer before eluting with 20 mM Tris•HCl (pH 8.0), 500 mM NaCl, 250 mM imidazole, and 10% (v/v) glycerol. Protein-containing fractions were analyzed by SDS-PAGE, pooled, and exchanged into 20 mM Tris•HCl (pH 7.7), 500 mM NaCl, and 10% (v/v) glycerol prior to concentration using a 50 mL Amicon stirred cell fitted with a 30 kDa molecular weight cut-off (MWCO) polyethersulfone filter (Millipore). MsuC was aliquoted, frozen in liquid N_2, and stored at −80 °C for assays. For crystallography, MsuC was thawed and dialyzed against 50 mM Tris (pH 8.5), 10% (v/v) glycerol, and 1 mM DTT, prior to loading onto a 5 mL UnoSphereQ column (Bio-Rad) pre-equilibrated in the same buffer. Protein was eluted over a linear gradient from 0 to 500 mM NaCl, and protein-containing fractions were pooled, concentrated in a Vivaspin 20 (10 kDa MWCO) centrifugal concentrator (GE Healthcare), and loaded onto a HiLoad 16/600 Superdex 200 pg column (GE Healthcare) pre-equilibrated in 50 mM Tris (pH 8.0), 200 mM NaCl, 10% (v/v) glycerol, and 1 mM DTT. The eluted protein peak was concentrated, aliquoted, flash frozen in liquid N_2, and stored at −80 °C. Protein concentration was determined via the Bradford method [15].

2.3. Crystallography

MsuC crystallized at 18 °C via sitting-drop vapor diffusion against a reservoir of 0.1 M Tris (pH 8.5), 0.15 M $CaCl_2$, and 30% (w/v) PEG 3350. Drops contained 1 μL MsuC (5 mg mL^{-1}), 1 μL reservoir, and 0.5 μL 100% (v/v) glycerol. Crystals were cryoprotected in 0.1 M Tris (pH 8.5), 0.15 M $CaCl_2$, 30% (w/v) PEG 3350, 2 mM FMN, and 15% (v/v) glycerol for 48 h and flash cooled in liquid N_2. X-ray diffraction data were collected at beamline 24ID-E at the Advanced Photon Source, Argonne National Laboratory. Data were processed using XDS [16], and molecular replacement was performed in PHASER [17,18] using PDB 5XB8 [19] as a search model. Two molecules were placed within the asymmetric unit and submitted to PHENIX AutoBuild, which rebuilt 375 out of 395 residues per monomer. The resulting model was subjected to iterations of manual model building in COOT [20] with positional and B-factor refinement and simulated annealing in PHENIX [17]. NCS restraints were used and released in later rounds of refinement, and occupancies of alternate protein side chain conformations were optimized. The model was verified using composite omit electron density maps and Ramachandran analysis in MolProbity [21]. Data and model statistics are presented in Table S2. Model preparation and docking calculations were performed in BioLuminate 3.5 (Schrödinger). MsuC with FMN positioned from TdsC (PDB 5XDE) was completed by adding missing side chains using Prime [22,23] and was preprocessed to assign bond orders, charges and protonation states using the Protein Preparation Wizard [24]. Placed FMN was energy minimized to reduce steric clashes. The substrate MSI^- was built and structurally optimized using DFT in Jaguar [25] (B3LYP-D3 with Poisson Boltzmann finite element water solvation and the 6–31g**++ basis). Rigid body docking was performed using default settings in Glide [26,27]. Figures were generated using Chemdraw (PerkinElmer) and PyMOL (Schrödinger).

2.4. Detection of monooxygenase activity

Assay solutions (1 mL) contained 1 mM MSI^-, 2 μM FMN, 20 μM MsuC, 0.5 μM $MsuE_{Pflu}$, prepared as previously reported [12], catalase (bovine liver, 1000 U mL^{-1}), 50 mM KP_i (pH 7.5), and

100 mM NaCl. Reactions were initiated with a final concentration of 1 mM NADH and incubated at 30 °C, 100 rpm for 1 h. Urea (1 mL, 1 M) was added to quench enzyme activity. Solutions were lyophilized and subsequently dissolved in 0.5 mL D_2O, filtered through a 0.2 μm filter, and analyzed by ^{1}H NMR spectroscopy at 400 MHz using instrumentation maintained by the Department of Chemistry Instrumentation Facility at Massachusetts Institute of Technology.

3. Results

3.1. MsuC adopts a dehydrogenase superfamily fold

The 1.69 Å resolution crystal structure of MsuC adopts the acyl-CoA dehydrogenase fold [28,29], with an N-terminal α-domain (L9 – F118) containing five α-helices, a central β-domain (W119 – T222) comprised of two β-sheets, and a C-terminal α-domain (P223 – Y394) containing five α-helices (Fig. 2 and S1A,B). The final model is missing only the N-terminal affinity tag and the first eight residues of the MsuC coding sequence (M1 – T8) due to poor electron density. MsuC is most structurally similar to the dibenzothiophene (DBT) monooxygenases TdsC (r.m.s. deviation of 1.4 Å for 385 cα atoms) and DszC (r.m.s. deviation of 1.3 Å for 386 cα atoms), with 43% and 42% amino acid sequence identity, respectively (Figs. S1C and S2) [19,30–32]. TdsC and DszC are class D [13] sulfur assimilation proteins that catalyze sequential oxidations of sulfur within DBT (S^{-2}) to dibenzothiophene sulfoxide (DBTO, S^0) and dibenzothiophene sulfone ($DBTO_2$, S^{+2}) (Fig. 1).

The MsuC asymmetric unit contains a dimer, and crystallographic symmetry defines a dimer of dimers configuration, or homotetramer (Fig. 2), also observed in gel filtration (Fig. S1D). The tetramer buries 13,340 Å^2 of surface area [33], and contacts between MsuC chains are primarily established by the C-terminal α-domain. The quaternary structure of MsuC is consistent with DBT monooxygenases [19,30–32] and other class D flavin-dependent monooxygenases exhibiting the acyl-CoA dehydrogenase fold [34–37].

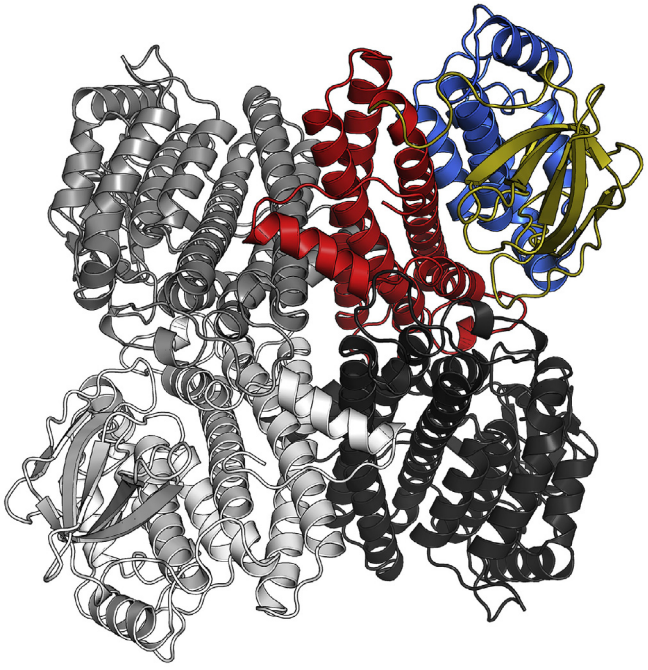

Fig. 2. Overall tetrameric structure of MsuC. Molecule A is colored with the N-terminal α-domain in blue, the β-domain in yellow, and the C-terminal α-domain in red. Remaining molecules are black, grey, and white. (For interpretation of the references to color in this figure legend, the reader is referred to the Web version of this article.)

3.2. MsuC demonstrates monooxygenase activity

Because of the sequence and structural similarity between DBT monooxygenases and MsuC, it was hypothesized that MsuC might be functionally similar to TdsC/DszC and mediate the formation of a S=O bond, specifically the oxidation of MSI^- (S^{+2}) to MS^- (S^{+4}) (Figs. 1 and 3). Furthermore, given the position of MsuC in the *msu* operon and its putative assignment as a dehydrogenase or oxygenase [3], we speculated that there might be an *in vivo* pathway for the synthesis of MS^- [38]. In order to test for the production of MS^- by MsuC, an assay was designed employing the NADH:FMN oxidoreductase $MsuE_{Pflu}$ [12]. Nonenzymatic oxidation of MSI^- to MS^- from futile coupling of $FMNH^-$ and O_2 has been observed *in vitro*, therefore, catalase was added to neutralize released H_2O_2 [39]. Finally, the flavin concentration was kept an order of magnitude lower than the monooxygenase to limit the formation of free $FMNH^-$ in solution.

The ^{1}H NMR spectrum of the endpoint assay shows near complete conversion of MSI^- to MS^- (Fig. 3 and Figs. S3 and S4). When MsuE or both MsuC and MsuE were omitted from the reaction, MSI^- was recovered, thus MsuC requires the FMN reductase MsuE, consistent with the function of this enzyme as a two-component flavin-dependent monooxygenase that catalyzes the 2 e^- oxidation of sulfur. As expected, when the monooxygenase component MsuC is omitted from the reaction, generated free $FMNH^-$ from MsuE and O_2 in solution are able to mediate product formation despite the presence of catalase, consistent with reported nonenzymatic oxidation of MSI^- [12]; importantly, near complete conversion of MSI^- to MS^- is only observed when the monooxygenase MsuC is included. It was speculated that DMSO might also be a substrate for MsuC, as the oxidation of DMSO to $DMSO_2$ would provide an *in vivo* pathway for the biochemical synthesis of the substrate for SfnG. However, an endpoint assay with DMSO showed no $DMSO_2$ formation, suggesting MsuC is specific for the S^{+2} oxyanion (Fig. S5).

3.3. MsuC contains a conserved flavin-binding site

The monooxygenase activity of MsuC suggests that MsuC contains an active site where both reduced FMN and MSI^- bind. Although crystals were soaked in cryoprotectant with FMN, no electron density for FMN was observed. Structural superimpositions of MsuC with the homologs TdsC and DszC (Fig. S6) [19,31] reveal that loops surrounding the active site are in a "closed" confirmation in the MsuC structure, suggesting why FMN soaking experiments were unsuccessful. Therefore, structural superimpositions of MsuC with the FMN-bound homologs TdsC (Fig. 4A) and DszC (Fig. S6) [19,31] were used to model FMN within the MsuC active site.

The proposed flavin-binding site in MsuC is located between both α-domains and the β-domain, and it shares several conserved residues with TdsC (Fig. 4B) and DszC (Fig. S7A) capable of interacting with the isoalloxazine ring. N5 of the modeled FMN is positioned within hydrogen-bonding distance of S149 in MsuC, and N121 is poised to interact with N3 and O4. F147 and W188 form van der Waals contacts with the *si*-face of the isoalloxazine ring. Interestingly, N124 in MsuC replaces a serine residue in TdsC and DszC observed within hydrogen-bonding distance of the N1 position, which could interact with either the protonated or deprotonated forms of reduced flavin. N124 is positioned away from the modeled flavin in MsuC and would need to undergo a conformational change to interact.

Residues proposed to interact with the phosphoribityl portion of FMN are primarily from the C-terminal α–domains of two adjacent protomers (Fig. 4A). The C-terminal carboxylate (S395) engages in a

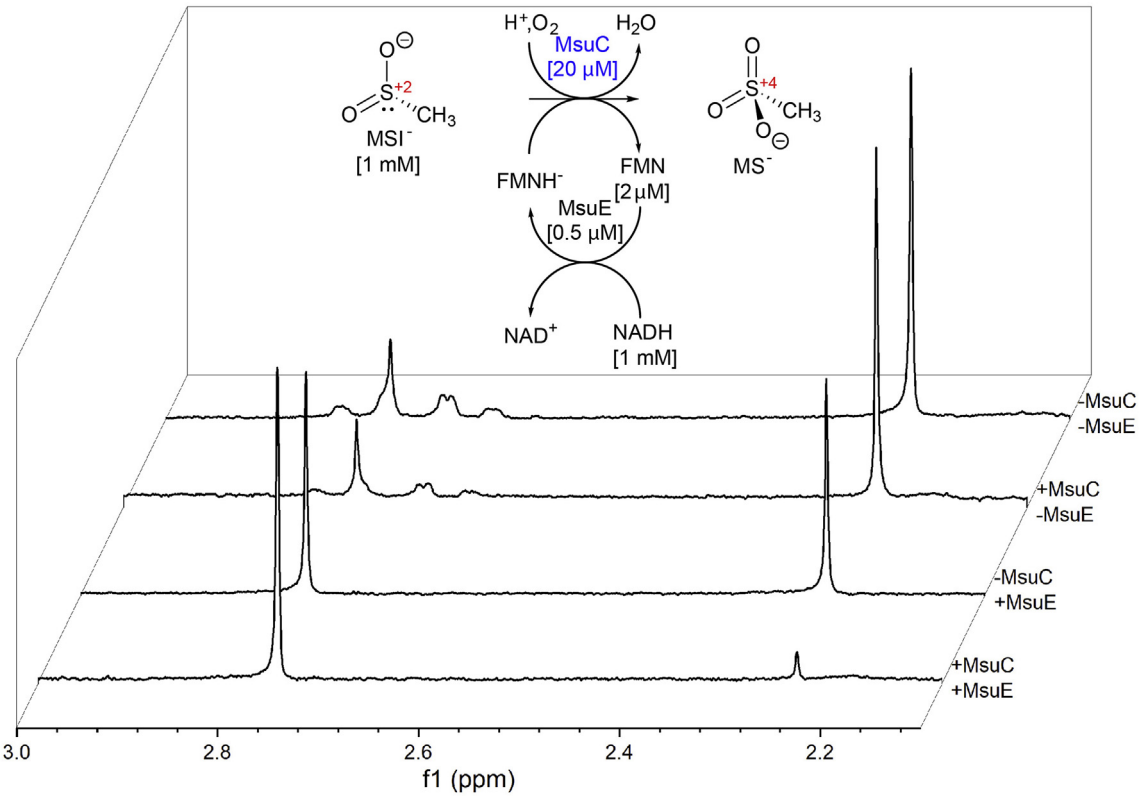

Fig. 3. MsuC activity determined by ^{1}H NMR spectroscopy. MSI^{-} and MS^{-} resonate at δ 2.2 ppm and δ 2.7 ppm, respectively. Nearly complete conversion of MSI^{-} to MS^{-} is observed in the presence of both MsuC and MsuE. Approximately half conversion is observed in the absence of MsuC, attributed to nonenzymatic oxidation of free FMNH^{-}. MSI^{-} is largely recovered in the absence of MsuE (or all enzymes), as is unreacted NADH (four broad resonances between δ 2.8 ppm and δ 2.6 ppm). A small amount of background oxidation of MSI^{-} to MS^{-} is observed under the reported assay conditions.

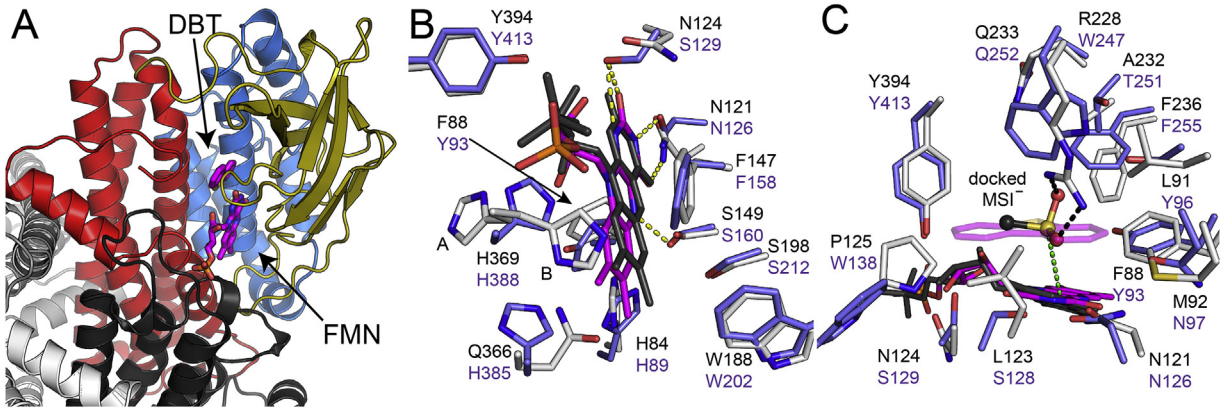

Fig. 4. Putative substrate-binding sites in MsuC. (A) Putative binding sites are located within each MsuC molecule, with DBT and FMN obtained from superimposition with TdsC (PDB ID 5XDE). MsuC is colored as in Fig. 2, with the C-terminal α–domain of the adjacent protomer in dark grey. (B) Superimposition of MsuC (grey) and TdsC (purple) identifies residues proposed to interact with FMN. As F147 is disordered in chain A of MsuC, chain B is shown. (C) Molecular docking of MSI^{-} determines a possible binding site. DBT is shown with transparent sticks to better visualize docked MSI^{-} in ball-and-stick. Residue labels are black for MsuC and purple for TdsC. Nitrogens are blue; oxygens are red; sulfurs are yellow; phosphorus atoms are orange; DBT and FMN carbons from TdsC are magenta; modeled and energy minimized FMN is dark grey; docked MSI^{-} carbon is dark grey; MsuC carbons are grey; TdsC carbons are purple; displayed hydrogen-bonding distances are colored black for MsuC and yellow for TdsC; and the FMN C4a–MSI^{-} sulfur distance is green. Alignment with DszC is omitted for clarity but included in Fig. S7. (For interpretation of the references to color in this figure legend, the reader is referred to the Web version of this article.)

bidentate hydrogen-bonding interaction with R316 (Fig. S8), and the penultimate Y394 is placed near the FMN ribityl moiety (Fig. 4B). However, higher B-factor values and residual negative difference electron density for Y394 and S395 suggest these residues are not positioned fully in the absence of bound FMN. Lastly, H369 is located further away from the modeled FMN and is observed in two alternate conformations, one of which corresponds more closely to the position of the analogous histidine in TdsC and DszC. Taken together, slight movements of residues within the C-terminal α-domain likely will accompany FMN binding.

3.4. MsuC contains a methanesulfinate binding site

Studies docking MSI^- into the proposed MsuC active site place MSI^- below the plane of the isoalloxazine ring (Fig. 4C and Fig. S7B), as observed for DBT and DBTO binding in structures of TdsC [19]. This docked pose positions the MSI^- sulfur atom 5.6 Å from the flavin C4a position, consistent with sulfur oxidation by MsuC. The two oxygen atoms of MSI^- are positioned near positively charged R228, poised to stabilize the negative charge on MSI^-. Two additional polar residues, N121 and N124, are located nearby and proposed to interact with the flavin isoalloxazine ring, and the rest of the binding site is of hydrophobic character. The protein C-terminal residues constitute one face of the MSI^- binding site; therefore, Y394 is positioned to interact with both MSI^- and the flavin, as detailed above.

4. Discussion

Here, we report that MsuC is the enzyme responsible for the conversion of MSI^- to MS^-, a reaction previously attributed to non-enzymatic chemical oxidation. MsuC is a two-component flavin-dependent monooxygenase that functions as the second enzyme required for the assimilation of $DMSO_2$ to sulfite, revealing a novel step in bacterial metabolism of organosulfur compounds. $DMSO_2$ is deposited from the chemical oxidation of atmospheric DMS, thus the metabolic pathway from $DMSO_2$ to SO_3^{2-} is important to the global cycling of sulfur. Indeed, it has been shown that the regulation of *sfnG* and *msuEDC* by enhancer-binding protein SfnR2 is directly correlated to DMS assimilation in *P. aeruginosa* PAO1 [40]. Endoh and coworkers first identified SfnR in 2003 as the last gene in the *sfnECR* operon responsible for the regulation of DMS metabolism in *P. putida DS1* [41], but purified recombinant enzymes shown to mediate the biochemical conversion of DMS to DMSO or of DMSO to $DMSO_2$ in any species of Pseudomonads have not been reported. Proteins connecting DMS to the *in vivo* synthesis of $DMSO_2$ have been genetically characterized as two-component flavin-dependent assimilatory DMS and DMSO S-monooxygenases [42], and efforts to study the putative S-monooxygenases *in vitro* are currently underway.

Our studies reveal similarities and intriguing differences between MsuC and the DBT monooxygenases DszC/TdsC and provide additional information for the structure and function of class D flavin-dependent monooxygenases [13]. Both DszC and TdsC are capable of catalyzing successive oxygenation reactions (DBT → DBTO → $DBTO_2$), yet MsuC is unable to convert DMSO to $DMSO_2$. The MsuC structure suggests why. Although predicted FMN-binding residues are highly similar in these homologous sulfur assimilation proteins, residues involved in organosulfur substrate binding are not. The proposed MSI^- site has evolved to stabilize the binding of a negatively charged molecule, whereas DMSO is a neutral molecule. Additional structural and biochemical studies are currently under way to elucidate the mechanism and promiscuity of this system.

Structure deposition

The MsuC coordinates and structure factors (PDB ID 6UUG) have been deposited to the Protein Data Bank (http://wwpdb.org/).

Sources of funding

This work was supported by the National Science Foundation, United States (NSF) [1807480 to DKW and DPD]. Any opinions, findings and conclusions or recommendations expressed in this material are those of the author(s) and do not necessarily reflect the views of the NSF.

Declaration of competing interest

The authors declare that there are no conflicts of interest.

Acknowledgments

The authors kindly acknowledge the MIT Structural Biology Core facility and Staff Scientist Robert Grant. This work used NE-CAT beamlines (GM124165) and an Eiger detector (S10OD021527) at the APS (DE-AC02-06CH11357).

Appendix A. Supplementary data

Supplementary data to this article can be found online at https://doi.org/10.1016/j.bbrc.2019.11.008.

Transparency document

Transparency document related to this article can be found online at https://doi.org/10.1016/j.bbrc.2019.11.008.

References

[1] E. Aguilar-Barajas, C. Diaz-Perez, M.I. Ramirez-Diaz, H. Riveros-Rosas, C. Cervantes, Bacterial transport of sulfate, molybdate, and related oxyanions, Biometals 24 (2011) 687–707, https://doi.org/10.1007/s10534-011-9421-x.
[2] E. Eichhorn, J.R. van der Ploeg, M.A. Kertesz, T. Leisinger, Characterization of α-ketoglutarate-dependent taurine dioxygenase from *Escherichia coli*, J. Biol. Chem. 272 (1997) 23031–23036, https://doi.org/10.1074/jbc.272.37.23031.
[3] M.A. Kertesz, K. Schmidt-Larbig, T. Wuest, A novel reduced flavin mononucleotide-dependent methanesulfonate sulfonatase encoded by the sulfur-regulated *msu* operon of *Pseudomonas aeruginosa*, J. Bacteriol. 181 (1999) 1464–1473.
[4] E. Eichhorn, J.R. van der Ploeg, T. Leisinger, Characterization of a two-component alkanesulfonate monooxygenase from *Escherichia coli*, J. Biol. Chem. 274 (1999) 26639–26646, https://doi.org/10.1074/jbc.274.38.26639.
[5] A.R.J. Curson, J.D. Todd, M.J. Sullivan, A.W.B. Johnston, Catabolism of dimethylsulphoniopropionate: microorganisms, enzymes and genes, Nat. Rev. Microbiol. 9 (2011) 849–859, https://doi.org/10.1038/nrmicro2653.
[6] O. Carrion, A.R.J. Curson, D. Kumaresan, Y. Fu, A.S. Lang, E. Mercade, J.D. Todd, A novel pathway producing dimethylsulphide in bacteria is widespread in soil environments, Nat. Commun. 6 (2015) 1–8, https://doi.org/10.1038/ncomms7579.
[7] R. Bentley, T.G. Chasteen, Environmental VOSCs–formation and degradation of dimethyl sulfide, methanethiol and related materials, Chemosphere 55 (2004) 291–317, https://doi.org/10.1016/j.chemosphere.2003.12.017.
[8] R. Boden, L.P. Hutt, Bacterial metabolism of C_1 sulfur compounds, in: F. Rojo (Ed.), Aerobic Utilization of Hydrocarbons, Oils and Lipids, Handbook of Hydrocarbon and Lipid Microbiology, Springer Nature, Switzerland AG, 2019, pp. 1–43, https://doi.org/10.1007/978-3-319-39782-5_9-1.
[9] B. Lei, S.-C. Tu, Gene overexpression, purification, and identification of a desulfurization enzyme from *Rhodococcus* sp. strain IGTS8 as a sulfide/sulfoxide monooxygenase, J. Bacteriol. 178 (1996) 5699–5705, https://doi.org/10.1128/jb.178.19.5699-5705.1996.
[10] S. Adak, T.P. Begley, Dibenzothiophene catabolism proceeds via a flavin-N5-oxide intermediate, J. Am. Chem. Soc. 138 (2016) 6424–6426, https://doi.org/10.1021/jacs.6b00583.
[11] R. Boden, E. Borodina, A.P. Wood, D.P. Kelly, J.C. Murrell, H. Schafer, Purification and characterization of dimethylsulfide monooxygenase from *Hyphomicrobium sulfonivorans*, J. Bacteriol. 193 (2011) 1250–1258, https://doi.org/10.1128/JB.00977-10.
[12] D.K. Wicht, The reduced flavin-dependent monooxygenase SfnG converts dimethylsulfone to methanesulfinate, Arch. Biochem. Biophys. 604 (2016) 159–166, https://doi.org/10.1016/j.abb.2016.07.001.
[13] M.M.E. Huijbers, S. Montersino, A.H. Westphal, D. Tischler, W.J.H. van Berkel, Flavin dependent monooxygenases, Arch. Biochem. Biophys. 544 (2014) 2–17, https://doi.org/10.1016/j.abb.2013.12.005.
[14] H.R. Ellis, The FMN-dependent two-component monooxygenase systems, Arch. Biochem. Biophys. 497 (2010) 1–12, https://doi.org/10.1016/j.abb.2010.02.007.
[15] M.M. Bradford, A rapid and sensitive method for the quantitation of microgram quantities of protein utilizing the principle of protein-dye binding, Anal. Biochem. 72 (1976) 248–254, https://doi.org/10.1016/0003-2697(76)90527-3.
[16] W. Kabsch, XDS, Acta Crystallogr. Sect. D Biol. Crystallogr. 66 (2010) 125–132,

https://doi.org/10.1107/s0907444909047337.
[17] P.D. Adams, P.V. Afonine, G. Bunkoczi, V.B. Chen, I.W. Davis, N. Echols, J.J. Headd, L.W. Hung, G.J. Kapral, R.W. Grosse-Kunstleve, A.J. McCoy, N.W. Moriarty, R. Oeffner, R.J. Read, D.C. Richardson, J.S. Richardson, T.C. Terwilliger, P.H. Zwart, PHENIX: a comprehensive Python-based system for macromolecular structure solution, Acta Crystallogr. Sect. D Biol. Crystallogr. 66 (2010) 213–221, https://doi.org/10.1107/S0907444909052925.
[18] A.J. McCoy, R.W. Grosse-Kunstleve, P.D. Adams, M.D. Winn, L.C. Storoni, R.J. Read, Phaser crystallographic software, J. Appl. Crystallogr. 40 (2007) 658–674, https://doi.org/10.1107/S0021889807021206.
[19] T. Hino, H. Hamamoto, H. Suzuki, H. Yagi, T. Ohshiro, S. Nagano, Crystal structures of TdsC, a dibenzothiophene monooxygenase from the thermophile *Paenibacillus* sp. A11-2, reveal potential for expanding its substrate selectivity, J. Biol. Chem. 292 (2017) 15804–15813, https://doi.org/10.1074/jbc.M117.788513.
[20] P. Emsley, K. Cowtan, Coot: model-building tools for molecular graphics, Acta Crystallogr. Sect. D Biol. Crystallogr. 60 (2004) 2126–2132, https://doi.org/10.1107/S0907444904019158.
[21] V.B. Chen, W.B. Arendall III, J.J. Headd, D.A. Keedy, R.M. Immormino, G.J. Kapral, L.W. Murray, J.S. Richardson, D.C. Richardson, MolProbity: all-atom structure validation for macromolecular crystallography, Acta Crystallogr. Sect. D Biol. Crystallogr. 66 (2010) 12–21, https://doi.org/10.1107/S0907444909042073.
[22] M.P. Jacobson, D.L. Pincus, C.S. Rapp, T.J. Day, B. Honig, D.E. Shaw, R.A. Friesner, A hierarchical approach to all-atom protein loop prediction, Proteins 55 (2004) 351–367, https://doi.org/10.1002/prot.10613.
[23] M.P. Jacobson, R.A. Friesner, Z. Xiang, B. Honig, On the role of the crystal environment in determining protein side-chain conformations, J. Mol. Biol. 320 (2002) 597–608, https://doi.org/10.1016/s0022-2836(02)00470-9.
[24] G.M. Sastry, M. Adzhigirey, T. Day, R. Annabhimoju, W. Sherman, Protein and ligand preparation: parameters, protocols, and influence on virtual screening enrichments, J. Comput. Aided Mol. Des. 27 (2013) 221–234, https://doi.org/10.1007/s10822-013-9644-8.
[25] A.D. Bochevarov, E. Harder, T.F. Hughes, J.R. Greenwood, D.A. Braden, D.M. Philipp, D. Rinaldo, M.D. Halls, J. Zhang, R.A. Friesner, Jaguar: a high-performance quantum chemistry software program with strengths in life and materials sciences, Int. J. Quantum Chem. 113 (2013) 2110–2142, https://doi.org/10.1002/qua.24481.
[26] R.A. Friesner, J.L. Banks, R.B. Murphy, T.A. Halgren, J.J. Klicic, D.T. Mainz, M.P. Repasky, E.H. Knoll, M. Shelley, J.K. Perry, D.E. Shaw, P. Francis, P.S. Shenkin, Glide: a new approach for rapid, accurate docking and scoring. 1. Method and assessment of docking accuracy, J. Med. Chem. 47 (2004) 1739–1749, https://doi.org/10.1021/jm0306430.
[27] T.A. Halgren, R.B. Murphy, R.A. Friesner, H.S. Beard, L.L. Frye, W.T. Pollard, J.L. Banks, Glide: a new approach for rapid, accurate docking and scoring. 2. Enrichment factors in database screening, J. Med. Chem. 47 (2004) 1750–1759, https://doi.org/10.1021/jm030644s.
[28] J.-J.P. Kim, J. Wu, Structure of the medium-chain acyl-CoA dehydrogenase from pig liver mitochondria at 3-Å resolution, Proc. Natl. Acad. Sci. U. S. A. 85 (1988) 6677–6681, https://doi.org/10.1073/pnas.85.18.6677.
[29] J.-J.P. Kim, R. Miura, Acyl-CoA dehydrogenases and acyl-CoA oxidases. Structural basis for mechanistic similarities and differences, Eur. J. Biochem. 271 (2004) 483–493, https://doi.org/10.1046/j.1432-1033.2003.03948.x.
[30] S. Liu, C. Zhang, T. Su, T. Wei, D. Zhu, K. Wang, Y. Huang, Y. Dong, K. Yin, S. Xu, P. Xu, L. Gu, Crystal structure of DszC from *Rhodococcus* sp. XP at 1.79 Å, Proteins 82 (2014) 1708–1720, https://doi.org/10.1002/prot.24525.
[31] L.J. Guan, W.C. Lee, S. Wang, T. Ohshiro, Y. Izumi, J. Ohtsuka, M. Tanokura, Crystal structures of apo-DszC and FMN-bound DszC from *Rhodococcus erythropolis* D-1, FEBS J. 282 (2015) 3126–3135, https://doi.org/10.1111/febs.13216.
[32] L. Zhang, X. Duan, D. Zhou, Z. Dong, K. Ji, W. Meng, G. Li, X. Li, H. Yang, T. Ma, Z. Rao, Structural insights into the stabilization of active, tetrameric DszC by its C-terminus, Proteins 82 (2014) 2733–2743, https://doi.org/10.1002/prot.24638.
[33] E. Krissinel, K. Henrick, Inference of macromolecular assemblies from crystalline state, J. Mol. Biol. 372 (2007) 774–797, https://doi.org/10.1016/j.jmb.2007.05.022.
[34] A. Alfieri, F. Fersini, N. Ruangchan, M. Prongjit, P. Chaiyen, A. Mattevi, Structure of the monooxygenase component of a two-component flavoprotein monooxygenase, Proc. Natl. Acad. Sci. U. S. A. 104 (2007) 1177–1182, https://doi.org/10.1073/pnas.0608381104.
[35] S.-H. Kim, T. Hisano, K. Takeda, W. Iwasaki, A. Ebihara, K. Miki, Crystal structure of the oxygenase component (HpaB) of the 4-hydroxyphenylacetate 3-monooxygenase from *Thermus thermophilus* HB8, J. Biol. Chem. 282 (2007) 33107–33117, https://doi.org/10.1074/jbc.M703440200.
[36] N.A. Bruender, J.B. Thoden, H.M. Holden, X-ray structure of KijD3, a key enzyme involved in the biosynthesis of D-kijanose, Biochemistry 49 (2010) 3517–3524, https://doi.org/10.1021/bi100318v.
[37] R.P. Hayes, B.N. Webb, A.K. Subramanian, M. Nissen, A. Popchock, L. Xun, C. Kang, Structural and catalytic differences between two $FADH_2$-dependent monooxygenases: 2,4,5-TCP 4-monooxygenase (TftD) from *Burkholderia cepacia* AC1100 and 2,4,6-TCP 4-monooxygenase (TcpA) from *Cupriavidus necator* JMP134, Int. J. Mol. Sci. 13 (2012) 9769–9784, https://doi.org/10.3390/ijms13089769.
[38] D.P. Kelly, J.C. Murrell, Microbial metabolism of methanesulfonic acid, Arch. Microbiol. 172 (1999) 341–348, https://doi.org/10.1007/s002030050770.
[39] V. Massey, Activation of molecular oxygen by flavins and flavoproteins, J. Biol. Chem. 269 22459-22462.
[40] B.R. Lundgren, Z. Sarwar, K.S. Feldman, J.M. Shoytush, C.T. Nomuraa, SfnR2 regulates dimethyl sulfide-related utilization in *Pseudomonas aeruginosa* PAO1, J. Bacteriol. 201 (2019) 1–22, https://doi.org/10.1128/JB.00606-18.
[41] T. Endoh, H. Habe, T. Yoshida, H. Nojiri, T. Omori, A CysB-regulated and σ^{54}-dependent regulator, SfnR, is essential for dimethyl sulfone metabolism of *Pseudomonas putida* strain DS1, Microbiology 149 (2003) 991–1000, https://doi.org/10.1099/mic.0.26031-0.
[42] H. Habe, A. Kouzuma, T. Endoh, T. Omori, H. Yamane, H. Nojiri, Transcriptional regulation of the sulfate-starvation-induced gene *sfnA* by a σ^{54}-dependent activator of *Pseudomonas putida*, Microbiology 153 (2007) 3091–3098, https://doi.org/10.1099/mic.0.2007/008151-0.